Inversion for two sets of fracture weaknesses using differences between azimuthal reflection coefficients –Theory and synthetic examples

Huaizhen Chen*, Junxiao Li and Kristopher A. Innanen

ABSTRACT

We first express stiffness parameters in terms of two sets of fracture weaknesses for the case of fractured rock consisting of two orthogonal sets of vertical fractures. Using perturbations in these stiffness parameters for the case of an interface separating an isotropic layer and a fractured layer, we derive a linearized P-to-P reflection coefficient as a function of two sets of fracture weakness, and we present differences in azimuthal reflection coefficients in terms of the tangential fracture weaknesses and the normal fracture weakness intercepts. Using the differences in azimuthal reflection coefficients, we establish an approach of estimating the tangential fracture weaknesses and the normal fracture weakness intercepts following a Bayesian framework. Synthetic tests confirm that the unknown parameter vector involving the tangential fracture weaknesses and the normal fracture weakness intercepts is estimated stably and reliably in the case of signal-to-noise ratio of 2.

INTRODUCTION

Natural fractures in subsurface layers are complex. Determination of fracture networks using observed seismic data sets are important for reservoir characterization. Bakulin et al. (2000a) propose how to compute stiffness parameters in rocks that contain only a single set of vertical fractures, which is equivalent to a horizontal transversely isotropic medium (HTI); and Bakulin et al. (2000b) extend the research to more complicated and realistic models that contain two sets of vertical fractures orthogonal to each other, which is a orthorhombic medium.

Following Bakulin et al. (2000b), we first proposed simplified and approximate stiffness parameters of the orthorhombic medium in terms of two sets of fracture weaknesses. In the case of an interface separating an isotropic layer and a fractured layer we express perturbations in stiffness parameters. Using the scattering proposed by Shaw and Sen (2004), which is a function of perturbation in stiffness matrix, we derive a linearized reflection coefficient again in terms of two sets of fracture weakness. We express difference in azimuthal reflection coefficients in terms of fracture weaknesses, and using the relationship between fracture weaknesses and fracture density, we re-express the reflection coefficient difference as a function of fracture density.

Based on the derived expression of difference in azimuthal reflection coefficients, we establish an inversion approach of employing azimuthal seismic amplitude differences to estimate fracture densities. Synthetic seismic data, which are added with Gaussian random noise, are utilized to testify the proposed inversion approach.

THEORY AND METHOD

In the present study, we focus on the case of fractured rock that is composed of two orthogonal sets of vertical fractures embedded in an isotropic background, as plotted in Figure 1.

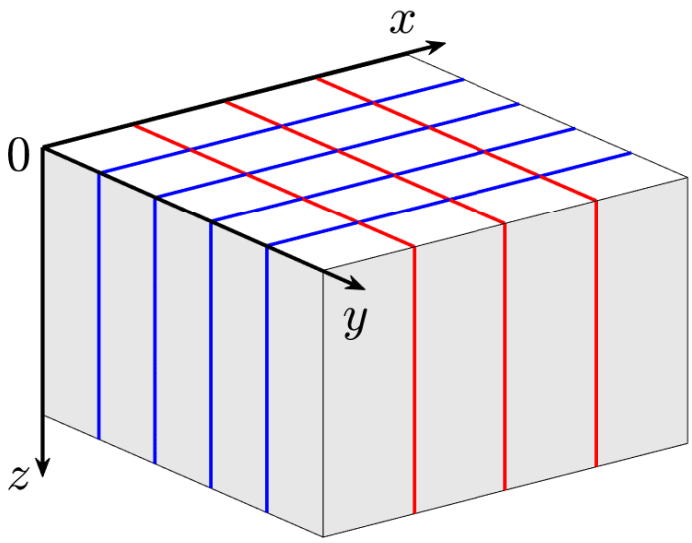

FIG. 1. A model of fractured rock consisting of two orthogonal sets of vertical fractures.

In this section we explain how to obtain simplified and approximate stiffness matrix of the fractured rock. Using the simplified stiffness matrix we will derive a linearized P-to-P reflection coefficient as a function of fracture weaknesses. Based on the linearized reflection coefficient, we will establish an approach and workflow of employing observed seismic data to estimate fracture weaknesses.

Simplified stiffness matrix of fractured rocks

Under the assumption of fractures being rotationally invariant and the background being isotropic, Bakulin et al. (2000b) proposed the effective stiffness matrix of the rock that

contains two orthogonal sets of vertical fractures

$$\begin{aligned}\mathbf{C} &= \begin{bmatrix} C_{11} & C_{12} & C_{13} & 0 & 0 & 0 \\ C_{12} & C_{22} & C_{23} & 0 & 0 & 0 \\ C_{13} & C_{23} & C_{33} & 0 & 0 & 0 \\ 0 & 0 & 0 & C_{44} & 0 & 0 \\ 0 & 0 & 0 & 0 & C_{55} & 0 \\ 0 & 0 & 0 & 0 & 0 & C_{66} \end{bmatrix} \\ &= \begin{bmatrix} \frac{Ml_1m_3}{d} & \frac{\lambda l_1m_1}{d} & \frac{\lambda l_1m_2}{d} & 0 & 0 & 0 \\ \frac{\lambda l_1m_1}{d} & \frac{Ml_3m_1}{d} & \frac{\lambda l_2m_1}{d} & 0 & 0 & 0 \\ \frac{\lambda l_1m_2}{d} & \frac{\lambda l_2m_1}{d} & \frac{M(l_3m_3-l_4)}{d} & 0 & 0 & 0 \\ 0 & 0 & 0 & \mu\left(1-\delta_{T2}\right) & 0 & 0 \\ 0 & 0 & 0 & 0 & \mu\left(1-\delta_{T1}\right) & 0 \\ 0 & 0 & 0 & 0 & 0 & \mu\frac{(1-\delta_{T1})(1-\delta_{T2})}{1-\delta_{T1}\delta_{T2}} \end{bmatrix}, \end{aligned} \tag{1}$$

where λ and μ are Lamé parameters of the isotropic background, $M = \lambda + 2\mu$, and

$$\begin{aligned} &l_1 = 1-\delta_{N1},\ l_2 = 1-(1-2g)\,\delta_{N1},\ l_3 = 1-(1-2g)^2\,\delta_{N1}, \\ &l_4 = 4\,(1-2g)^2\,g^2\delta_{N1}\delta_{N2},\ m_1 = 1-\delta_{N2},\ m_2 = 1-(1-2g)\,\delta_{N2}, \\ &m_3 = 1-(1-2g)^2\,\delta_{N2},\ d = 1-(1-2g)^2\,\delta_{N1}\delta_{N2}, \end{aligned} \tag{2}$$

in which

$$g = \frac{\mu}{M}, \tag{3}$$

and δ_{N1}, δ_{N2}, δ_{T1} and δ_{T2} are the normal and tangential fracture weaknesses related to the orthogonal sets of vertical fractures (Bakulin et al., 2000b).

Under the assumptions that the normal and tangential fracture weaknesses are relatively small (i.e. $0 \le \delta_{N1}, \delta_{N2}, \delta_{T1}, \delta_{T2} < 1$), we neglect the term proportional to $\delta_{N1}\delta_{N2}$ and $\delta_{T1}\delta_{T2}$; hence, the stiffness parameters are simplified as

$$\begin{aligned} C_{11} &\approx M\left[1-\delta_{N1}-(1-2g)^2\,\delta_{N2}\right], \\ C_{12} &\approx \lambda\left(1-\delta_{N1}-\delta_{N2}\right), \\ C_{13} &\approx \lambda\left[1-\delta_{N1}-(1-2g)\,\delta_{N2}\right], \\ C_{22} &\approx M\left[1-(1-2g)^2\,\delta_{N1}-\delta_{N2}\right], \\ C_{23} &\approx \lambda\left[1-(1-2g)\,\delta_{N1}-\delta_{N2}\right], \\ C_{33} &\approx M\left[1-(1-2g)^2\,\delta_{N1}-(1-2g)^2\,\delta_{N2}\right], \\ C_{44} &= \mu\left(1-\delta_{T2}\right), \\ C_{55} &= \mu\left(1-\delta_{T1}\right), \\ C_{66} &\approx \mu\left(1-\delta_{T1}-\delta_{T2}\right). \end{aligned} \tag{4}$$

We next use a model of the middle Woodford shale (Far et al., 2013) to testify the accuracy of the simplified stiffness parameters. Table 1 shows elastic parameters (P- and S-wave velocities V_{P} and V_{S}, P- and S-wave moduli M and μ, and density ρ) of the isotropic background rock.

Table 1. Elastic parameters of the isotropic background rock (Far et al., 2013)

V_{P} (km/s)	V_{S} (km/s)	ρ (g/cm^3)	M (GPa)	μ (GPa)
4.161	2.687	2.46	42.592	17.761

Given different values of δ_{N1}, δ_{N2}, δ_{T1} and δ_{T2}, we respectively calculate exact and approximate stiffness parameters using equations 1-4, and in Figure 2 we plot the relative difference between the exact and approximate results. We observe that in the case of fracture weaknesses being smaller than 0.3, the relative differences of stiffness parameters C_{11}, C_{13}, C_{22}, C_{23}, C_{33} and C_{66}, which are computed using the exact and approximate results, are less than 3%. Although the maximum relative difference of C_{12} approaches to 20% in the case of δ_{N1} and δ_{N2} being 0.3, most of its relative difference are less than 10%. We may conclude that the simplified stiffness parameters are acceptable in the case that two sets of fracture weaknesses are small.

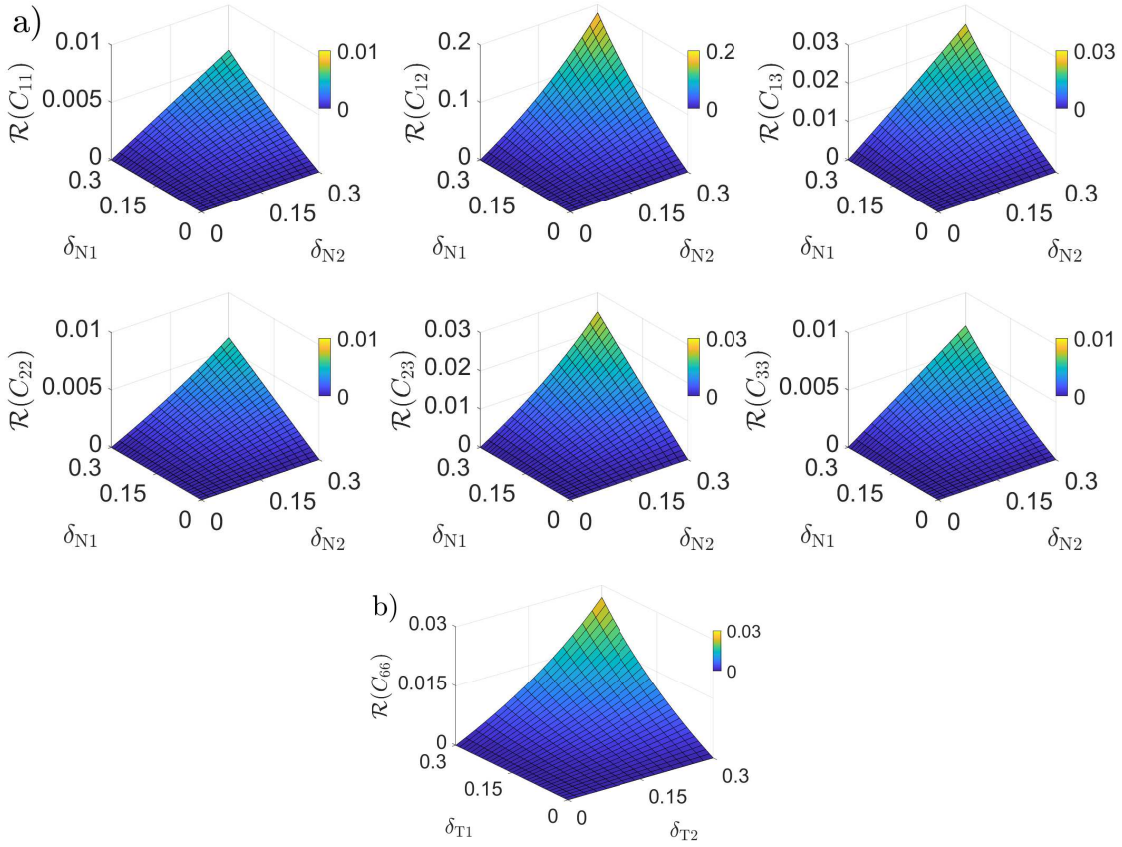

FIG. 2. Relative differences between exact and approximate results of stiffness parameters. The relative difference is computed as $\mathcal{R}(C_{ij}) = \left|\frac{C_{ij}^{\mathrm{approx}} - C_{ij}^{\mathrm{exact}}}{C_{ij}^{\mathrm{exact}}}\right|$, where C_{ij}^{approx} and C_{ij}^{exact} respectively represent approximate and exact results of stiffness parameter.

Derivation of P-to-P linearized reflection coefficient

Using the simplified stiffness parameters, we proceed to the derivation of a linearized reflection coefficient for an interface that separates an isotropic layer and a fractured layer. We first express perturbations in stiffness parameters across the interface as

$$
\begin{aligned}
\Delta C_{11} &\approx \Delta M - M\delta_{N1} - M\left(1-2g\right)^2\delta_{N2},\\
\Delta C_{12} &\approx \Delta\lambda - \lambda\delta_{N1} - \lambda\delta_{N2},\\
\Delta C_{13} &\approx \Delta\lambda - \lambda\delta_{N1} - \lambda\left(1-2g\right)\delta_{N2},\\
\Delta C_{22} &\approx \Delta M - M\left(1-2g\right)^2\delta_{N1} - M\delta_{N2},\\
\Delta C_{23} &\approx \Delta\lambda - \lambda\left(1-2g\right)\delta_{N1} - \lambda\delta_{N2},\\
\Delta C_{33} &\approx \Delta M - M\left(1-2g\right)^2\delta_{N1} - M\left(1-2g\right)^2\delta_{N2},\\
\Delta C_{44} &= \Delta\mu - \mu\delta_{T2},\\
\Delta C_{55} &= \Delta\mu - \mu\delta_{T1},\\
\Delta C_{66} &\approx \Delta\mu - \mu\delta_{T1} - \mu\delta_{T2},
\end{aligned}
\tag{5}
$$

where ΔM and $\Delta\mu$ are changes in P- and S-wave moduli across the interface, and we stress that in the perturbations we neglect the term that is proportional to $\Delta M\delta_{N1}$, $\Delta M\delta_{N2}$, $\Delta\lambda\delta_{N1}$, $\Delta\lambda\delta_{N2}$, $\Delta\mu\delta_{T1}$ and $\Delta\mu\delta_{T2}$ again under the assumptions that changes in both elastic parameters (M, μ, and λ) across the interface and two sets of fracture weaknesses are small.

Following Pšenčík and Gajewski (1998), Pšenčík and Vavryčuk (1998) and Vavryčuk and Pšenčík (1998), we derive the linearized P-to-P displacement reflection coefficient $R_{\mathrm{PP}}\left(\theta,\phi\right)$ as the sum of isotropic part $R_{\mathrm{PP}}^{\mathrm{iso}}\left(\theta\right)$ related to background media elastic parameters and anisotropic part $R_{\mathrm{PP}}^{\mathrm{ani}}\left(\theta,\phi\right)$ related to two sets of fracture weaknesses (Appendix A)

$$
\begin{aligned}
R_{\mathrm{PP}}\left(\theta,\phi\right) &= R_{\mathrm{PP}}^{\mathrm{iso}}\left(\theta\right) + R_{\mathrm{PP}}^{\mathrm{ani}}\left(\theta,\phi\right),\\
R_{\mathrm{PP}}^{\mathrm{iso}}\left(\theta\right) &= a_{\rho}\left(\theta\right)\frac{\Delta\rho}{\rho} + a_{M}\left(\theta\right)\frac{\Delta M}{M} + a_{\mu}\left(\theta\right)\frac{\Delta\mu}{\mu},\\
R_{\mathrm{PP}}^{\mathrm{ani}}\left(\theta,\phi\right) &= a_{N1}\left(\theta,\phi\right)\delta_{N1} + a_{N2}\left(\theta,\phi\right)\delta_{N2} + a_{T1}\left(\theta,\phi\right)\delta_{T1} + a_{T2}\left(\theta,\phi\right)\delta_{T2},
\end{aligned}
\tag{6}
$$

where

$$\begin{aligned}
a_\rho(\theta) =& \frac{1}{4}\frac{\cos 2\theta}{\cos^2\theta}, a_M(\theta) = \frac{1}{4}\sec^2\theta, a_\mu(\theta) = -2g\sin^2\theta, \\
a_{N1}(\theta,\phi) =& -\frac{1}{4}\left[(1-2g)\cos\theta + \cos^2\phi\sin\theta\tan\theta\right]^2 \\
& -\frac{(1-2g)}{2}\begin{bmatrix}\sec^2\theta - \frac{1}{2}\sin^2\phi\tan^2\theta \\ -g\left(2+\sin^2\phi\tan^2\theta\right)\end{bmatrix}\sin^2\theta\sin^2\phi, \\
a_{N2}(\theta,\phi) =& -\frac{1}{4}\left[(1-2g)\cos\theta + \sin^2\phi\sin\theta\tan\theta\right]^2 \\
& -\frac{(1-2g)}{2}\begin{bmatrix}\sec^2\theta - \frac{1}{2}\cos^2\phi\tan^2\theta \\ -g\left(2+\cos^2\phi\tan^2\theta\right)\end{bmatrix}\sin^2\theta\cos^2\phi, \\
a_{T1}(\theta,\phi) =& g\cos^2\phi\sin^2\theta\left(1-\sin^2\phi\tan^2\theta\right), \\
a_{T2}(\theta,\phi) =& g\sin^2\phi\sin^2\theta\left(1-\cos^2\phi\tan^2\theta\right),
\end{aligned} \tag{7}$$

in which θ is the incidence angle of P-wave, and ϕ is the azimuth, which is equal to zero in the (x, z) plane.

Inversion of azimuthal seismic amplitude differences for two sets of fracture weaknesses

Assuming we have seismic data sets of azimuthal angles $\phi_1 = 0$ and ϕ_j in hand, the difference between the reflection coefficients of ϕ_i and ϕ_j, $\Gamma_{\rm PP}$, is expressed as

$$\begin{aligned}
\Gamma_{\rm PP}(\theta,\phi_1,\phi_j) =& b_{N1}(\theta,\phi_1,\phi_j)\delta_{N1} + b_{N2}(\theta,\phi_1,\phi_j)\delta_{N2} \\
& + b_{T1}(\theta,\phi_1,\phi_j)\delta_{T1} + b_{T2}(\theta,\phi_1,\phi_j)\delta_{T2},
\end{aligned} \tag{8}$$

where

$$\begin{aligned}
b_{N1}(\theta,\phi_1,\phi_j) &= a_{N1}(\theta,\phi_j) - a_{N1}(\theta,\phi_1), \\
b_{N2}(\theta,\phi_1,\phi_j) &= a_{N2}(\theta,\phi_j) - a_{N2}(\theta,\phi_1), \\
b_{T1}(\theta,\phi_1,\phi_j) &= a_{T1}(\theta,\phi_j) - a_{T1}(\theta,\phi_1), \\
b_{T2}(\theta,\phi_1,\phi_j) &= a_{T2}(\theta,\phi_j) - a_{T2}(\theta,\phi_1).
\end{aligned} \tag{9}$$

In the difference between azimuthal reflection coefficients the effects of reflectivities of P- and S-wave moduli and density disappear, and the difference is mainly influenced by the fracture weaknesses. Based on the difference between azimuthal reflection coefficients, we proceed to the establishment of inversion approach of employing azimuthal seismic amplitude differences to estimate two sets of fracture weaknesses.

Following Bakulin et al. (2000a), we express the normal and tangential fracture weaknesses for fluid saturated fractures under the assumption that there are no interaction between two sets of fractures, which indicates that we may utilize fracture density e for each

set of fractures to compute the corresponding normal and tangential fracture weaknesses

$$\begin{aligned}\delta_{Ni} &= \frac{4e_i}{3g\,(1-g)\left[1+\frac{1}{\pi g(1-g)}\frac{K_f}{\mu\alpha_i}\right]},\\ \delta_{Ti} &= \frac{16e_i}{3\,(3-2g)},\end{aligned} \tag{10}$$

where e_i $(i = 1, 2)$ represents the fracture density of two sets of fractures, and α_i $(i = 1, 2)$ represents fracture aspect ratio. We emphasize that we assume the fluid is evenly filled in two sets of fractures. Given different values of fracture density, we plot how the normal fracture weakness δ_N varies with fracture aspect ratio α for the case of gas-bearing fractures in Figure 3 .

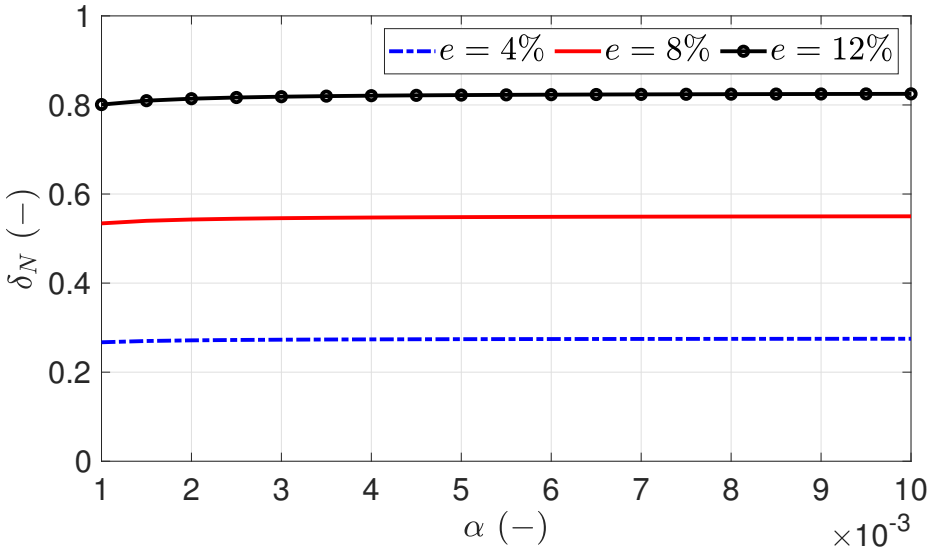

FIG. 3. Variations of normal fracture weakness with aspect ratio in the case of different values of fracture density (water saturation $s_{\mathrm{w}} = 50\%$).

In Figure 3 we observe that given a certain fracture density and water saturation for gas-bearing fractures the normal fracture weakness is approximately constant in the case of fracture aspect ratio being in $0.001 - 0.01$, which means α_i in equation 10 can be approximately written as α; and the normal fracture weakness changes significantly with fracture density. It may guide us to further express two sets of fracture weaknesses in terms of fracture density:

$$\begin{aligned}\delta_{N1} &= k_N\, e_1,\\ \delta_{N2} &= k_N\, e_2,\\ \delta_{T1} &= k_T\, e_1,\\ \delta_{T2} &= k_T\, e_2,\end{aligned} \tag{11}$$

where $k_N = \frac{4}{3g(1-g)\left[1+\frac{1}{\pi g(1-g)}\frac{K_f}{\mu\alpha}\right]}$, and $k_T = \frac{16}{3(3-2g)}$.

Substituting equation 11 into equation 8, we re-express the reflection coefficient difference as

$$\Gamma_{\mathrm{PP}}\left(\theta,\phi_1,\phi_j\right) = d_{NT1}\left(\theta,\phi_1,\phi_j\right)e_1 + d_{NT2}\left(\theta,\phi_1,\phi_j\right)e_2, \tag{12}$$

where

$$\begin{aligned} d_{NT1}\left(\theta,\phi_1,\phi_j\right) =& b_{N1}\left(\theta,\phi_1,\phi_j\right)k_N + b_{T1}\left(\theta,\phi_1,\phi_j\right)k_T, \\ d_{NT2}\left(\theta,\phi_1,\phi_j\right) =& b_{N2}\left(\theta,\phi_1,\phi_j\right)k_N + b_{T2}\left(\theta,\phi_1,\phi_j\right)k_T. \end{aligned} \tag{13}$$

The reflection coefficient difference is re-expressed as a function of fracture density, which may reduce the correlation between the normal and tangential fracture weaknesses due to fracture density. Using the re-expressed reflection coefficient difference, we next establish the approach and workflow of employing azimuthal seismic amplitude differences to estimate unknown parameters involving two fracture densities e_1 and e_2.

Assuming we have seismic angle gathers along azimuths ϕ_1, ϕ_2 and ϕ_3, the azimuthal seismic amplitude differences are expressed succinctly as

$$\mathbf{s} = \mathbf{G}\mathbf{x}, \tag{14}$$

where

$$\begin{aligned} \mathbf{s} =& \begin{bmatrix} s_{\mathrm{PP}}\left(\theta,\phi_1,\phi_2\right) \\ s_{\mathrm{PP}}\left(\theta,\phi_1,\phi_3\right) \end{bmatrix}, \\ \mathbf{G} =& \mathbf{W}\begin{bmatrix} d_{NT1}\left(\theta,\phi_1,\phi_2\right) & d_{NT2}\left(\theta,\phi_1,\phi_2\right) \\ d_{NT1}\left(\theta,\phi_1,\phi_3\right) & d_{NT2}\left(\theta,\phi_1,\phi_3\right) \end{bmatrix}, \\ \mathbf{x} =& \begin{bmatrix} e_1 \\ e_2 \end{bmatrix}, \end{aligned} \tag{15}$$

in which $\mathbf{W}$ represents the vector of wavelet extracted from observed seismic data, and s_{PP} represents seismic amplitude difference.

Using a Bayesian framework, we propose the objective function J in the case of assuming both the likelihood and priori probability distribution to be Gaussian distribution, which is expressed as

$$J = \frac{\left(\mathbf{s}-\mathbf{G}\mathbf{x}\right)^T\left(\mathbf{s}-\mathbf{G}\mathbf{x}\right)}{2\sigma^2_{\mathrm{noise}}} + \frac{\left(\mathbf{x}-\mathbf{x}_{\mathrm{prior}}\right)^T\left(\mathbf{x}-\mathbf{x}_{\mathrm{prior}}\right)}{2\mathbf{C}_{\mathrm{x}}}, \tag{16}$$

where the superscript T denotes the transpose of vector, $\mathbf{x}_{\mathrm{prior}}$ is the mean value of unknown parameter vector $\mathbf{x}$, $\sigma^2_{\mathrm{noise}}$ is the variance of Gaussian random noise, and $\mathbf{C}_{\mathrm{x}}$ is the covariance matrix of unknown parameters, which is given by

$$\mathbf{C}_{\mathrm{x}} \approx \begin{bmatrix} \sigma^2_{e_1} & \sigma_{e_1e_2} \\ \sigma_{e_1e_2} & \sigma^2_{e_2} \end{bmatrix}. \tag{17}$$

The solution of unknown parameter vector is given by

$$\mathbf{x} = \mathbf{x}_{\mathrm{prior}} + \mathbf{C}_{\mathrm{x}}\mathbf{G}^t\left(\mathbf{G}\mathbf{C}_{\mathrm{x}}\mathbf{G}^t + \sigma^2_{\mathrm{noise}}\mathbf{I}\right)^{-1}\left(\mathbf{s} - \mathbf{G}\,\mathbf{x}_{\mathrm{prior}}\right), \tag{18}$$

where $\mathbf{I}$ is the unit vector.

NUMERICAL EXAMPLES

We first utilize a layer-model to testify the stability and robustness of the proposed inversion approach. Figure 4 plots curves of fracture density and water saturation of the layer-model, and Figure 5 plots profiles of differences in azimuthal seismic data, which are generated using equations 12 and 14; and Ricker wavelet of dominant frequency 20 Hz is employed. Gaussian random noise is added into the synthetic seismic data difference (signal-to-noise ratio, SNR, is 2).

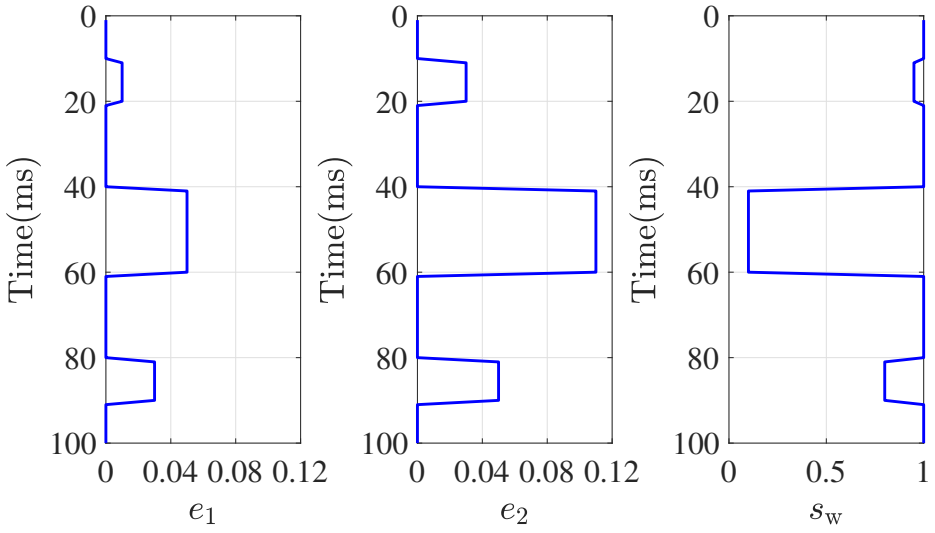

FIG. 4. Fracture density and water saturation of layer-model. The fluid is the mixture of water and gas.

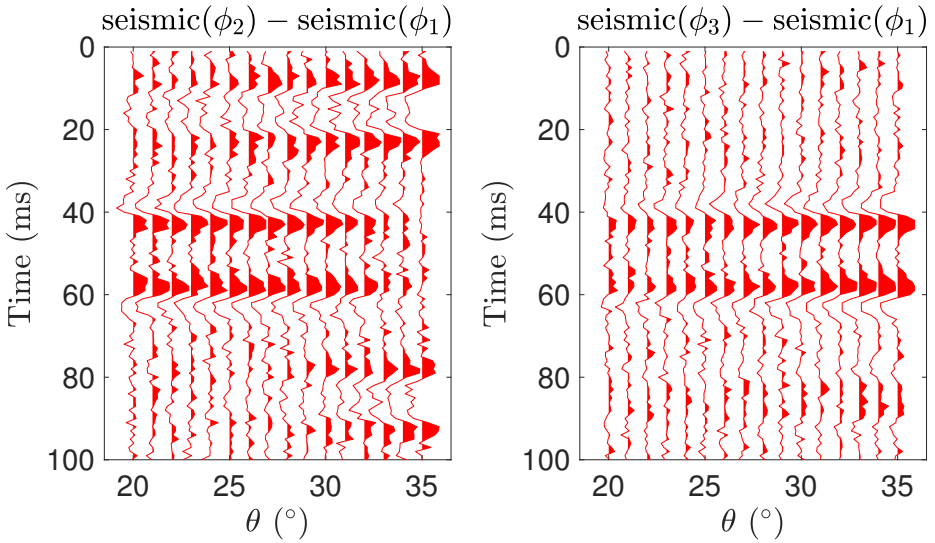

FIG. 5. Profiles of differences in azimuthal seismic data generated based on the derived reflection coefficient. $\phi_1 = 0$, $\phi_2 = 45°$, and $\phi_3 = 90°$

Using the proposed inversion approach, we implement the inversion of differences in azimuthal seismic data for two fracture densities, and in Figure 6 we plot comparisons between true values and inversion results of fracture density. We observe that there is a good match between the inversion result and true value of fracture density.

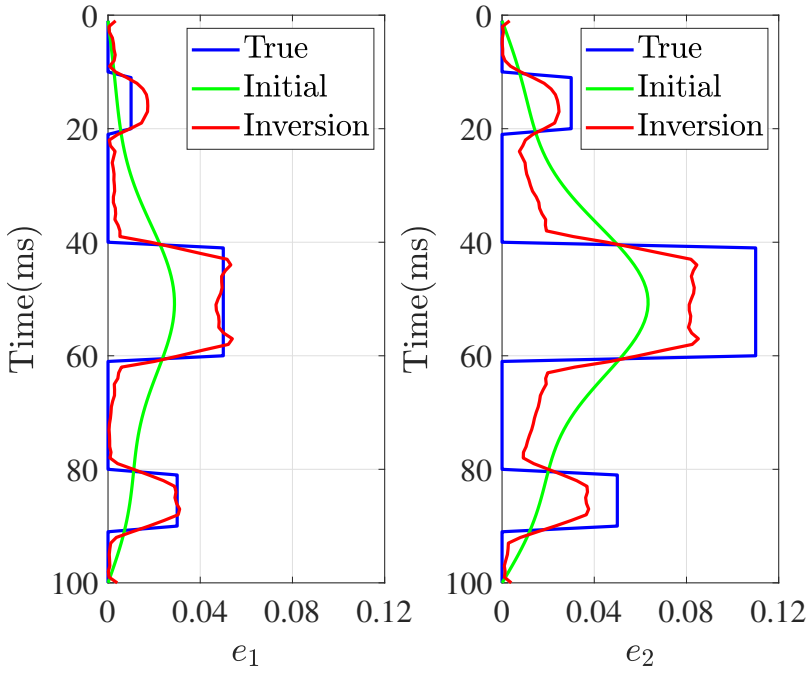

FIG. 6. Comparisons between inversion results and true values of fracture density. Green curve represents initial model of fracture density, which is a smoothed version of true value.

CONCLUSIONS

Beginning with simplifying stiffness parameters of orthorhombic media, we derive a linearized reflection coefficient in terms of two sets of fracture weaknesses, and we also express the difference in azimuthal reflection coefficients in terms of fracture weaknesses and fracture densities respectively. Using the derived expression of difference in azimuthal reflection coefficients, we establish an approach of employing differences in azimuthal seismic amplitude data to estimate fracture densities. Applying the approach to synthetic seismic data of signal-to-noise ratio (SNR) of 2, we may obtain stable inversion results of fracture densities, which is helpful for prediction of fracture networks and connectivity.

ACKNOWLEDGMENTS

We thank the sponsors of CREWES for continued support. This work was funded by CREWES industrial sponsors, and NSERC (Natural Science and Engineering Research Council of Canada) through the grant CRDPJ 461179-13. This work was also funded in part thanks to the Canada First Research Excellence Fund, and the Mitacs Accelerate grant *Responsible Development of Unconventional Hydrocarbon Reserves*.

APPENDIX A. DERIVATION OF LINEARIZED REFLECTION COEFFICIENT

Vavryčuk and Pšenčík (1998) proposed an expression of PP-wave reflection coefficient in the case that an interface separates two weakly arbitrary anisotropic media. Extending their PP-wave reflection coefficient to the case that an interface separating isotropic and fractured media, we rewrite the reflection coefficient as

$$
\begin{aligned}
R_{\mathrm{PP}}(\theta,\phi) \approx & \frac{\Delta\left(C_{33}/\rho\right)}{4{V_{\mathrm{P}}}^2}\left(1+\sin^2\theta\right)+\left(\frac{1}{2}-2g\sin^2\theta\right)\frac{\Delta\rho}{\rho} \\
& + \begin{bmatrix} \frac{\Delta(C_{13}/\rho+2C_{55}/\rho-C_{33}/\rho)}{2{V_{\mathrm{P}}}^2}\cos^2\phi \\ +\frac{\Delta(C_{23}/\rho+2C_{44}/\rho-C_{33}/\rho)}{2{V_{\mathrm{P}}}^2}\sin^2\phi \\ -2\frac{\Delta(C_{55}/\rho)}{{V_{\mathrm{P}}}^2}\cos^2\phi-2\frac{\Delta(C_{44}/\rho)}{{V_{\mathrm{P}}}^2}\sin^2\phi \end{bmatrix}\sin^2\theta \\
& + \begin{bmatrix} \frac{\Delta(C_{33}/\rho)}{4{V_{\mathrm{P}}}^2}+\frac{\Delta(C_{11}/\rho-C_{33}/\rho)}{4{V_{\mathrm{P}}}^2}\cos^4\phi \\ +\frac{\Delta(C_{22}/\rho-C_{33}/\rho)}{4{V_{\mathrm{P}}}^2}\sin^4\phi \\ +\frac{\Delta(C_{12}/\rho+2C_{66}/\rho-C_{33}/\rho)}{2{V_{\mathrm{P}}}^2}\sin^2\phi\cos^2\phi \end{bmatrix}\sin^2\theta\tan^2\theta \\
\approx & \frac{\Delta C_{33}}{4M}\left(1+\sin^2\theta\right)+\left(\frac{1}{2}-2g\sin^2\theta-\frac{C_{33}}{4M}-\frac{C_{33}}{4M}\sin^2\theta\right)\frac{\Delta\rho}{\rho} \\
& + \begin{bmatrix} \frac{\Delta(C_{13}+2C_{55}-C_{33})}{2M}\cos^2\phi \\ -\frac{(C_{13}+2C_{55}-C_{33})}{2M}\cos^2\phi\frac{\Delta\rho}{\rho} \\ +\frac{\Delta(C_{23}+2C_{44}-C_{33})}{2M}\sin^2\phi \\ -\frac{(C_{23}+2C_{44}-C_{33})}{2M}\sin^2\phi\frac{\Delta\rho}{\rho} \\ -2\frac{\Delta C_{55}}{M}\cos^2\phi+2\frac{C_{55}}{M}\cos^2\phi\frac{\Delta\rho}{\rho} \\ -2\frac{\Delta C_{44}}{M}\sin^2\phi+2\frac{C_{44}}{M}\sin^2\phi\frac{\Delta\rho}{\rho} \end{bmatrix}\sin^2\theta \\
& + \begin{bmatrix} \frac{\Delta C_{33}}{4M}-\frac{C_{33}}{4M}\frac{\Delta\rho}{\rho} \\ +\frac{\Delta(C_{11}-C_{33})}{4M}\cos^4\phi-\frac{(C_{11}-C_{33})}{4M}\cos^4\phi\frac{\Delta\rho}{\rho} \\ +\frac{\Delta(C_{22}-C_{33})}{4M}\sin^4\phi-\frac{(C_{22}-C_{33})}{4M}\sin^4\phi\frac{\Delta\rho}{\rho} \\ +\frac{\Delta(C_{12}+2C_{66}-C_{33})}{2M}\sin^2\phi\cos^2\phi \\ -\frac{(C_{12}+2C_{66}-C_{33})}{2M}\sin^2\phi\cos^2\phi\frac{\Delta\rho}{\rho} \end{bmatrix}\sin^2\theta\tan^2\theta.
\end{aligned}
\tag{A.1}
$$

Substituting equations 4 and 5 into equation A.1, we obtain the final expression of PP-wave reflection coefficient after some algebra

$$
\begin{aligned}
R_{\mathrm{PP}}(\theta,\phi) \approx & \frac{1}{4}\frac{\cos 2\theta}{\cos^2\theta}\frac{\Delta\rho}{\rho} + \frac{1}{4}\sec^2\theta\frac{\Delta M}{M} - 2g\sin^2\theta\frac{\Delta\mu}{\mu} \\
& - \left\{ \begin{array}{c} \frac{1}{4}\left[(1-2g)\cos\theta + \cos^2\phi\sin\theta\tan\theta\right]^2 \\ +\frac{(1-2g)}{2}\left[\sec^2\theta - \frac{1}{2}\sin^2\phi\tan^2\theta\right] \\ -g\left(2+\sin^2\phi\tan^2\theta\right) \end{array} \right\} \sin^2\theta\sin^2\phi \, \delta_{N1} \\
& - \left\{ \begin{array}{c} \frac{1}{4}\left[(1-2g)\cos\theta + \sin^2\phi\sin\theta\tan\theta\right]^2 \\ +\frac{(1-2g)}{2}\left[\sec^2\theta - \frac{1}{2}\cos^2\phi\tan^2\theta\right] \\ -g\left(2+\cos^2\phi\tan^2\theta\right) \end{array} \right\} \sin^2\theta\cos^2\phi \, \delta_{N2} \\
& + g\cos^2\phi\sin^2\theta\left(1-\sin^2\phi\tan^2\theta\right)\delta_{T1} \\
& + g\sin^2\phi\sin^2\theta\left(1-\cos^2\phi\tan^2\theta\right)\delta_{T2}.
\end{aligned}
\tag{A.2}
$$

REFERENCES

Bakulin, A., Grechka, V., and Tsvankin, I., 2000a, Estimation of fracture parameters from reflection seismic data—Part I: HTI model due to a single fracture set: Geophysics, **65**, No. 6, 1788–1802.

Bakulin, A., Grechka, V., and Tsvankin, I., 2000b, Estimation of fracture parameters from reflection seismic data—Part II: Fractured models with orthorhombic symmetry: Geophysics, **65**, No. 6, 1803–1817.

Far, M. E., Sayers, C. M., Thomsen, L., Han, D.-H., and Castagna, J. P., 2013, Seismic characterization of naturally fractured reservoirs using amplitude versus offset and azimuth analysis: Geophysical Prospecting, **61**, No. 2, 427–447.

Pšenčík, I., and Gajewski, D., 1998, Polarization, phase velocity, and NMO velocity of qP-waves in arbitrary weakly anisotropic media: Geophysics, **63**, No. 5, 1754–1766.

Pšenčík, I., and Vavryčuk, V., 1998, Weak contrast PP wave displacement R/T coefficients in weakly anisotropic elastic media: pure and applied geophysics, **151**, No. 2-4, 699–718.

Shaw, R. K., and Sen, M. K., 2004, Born integral, stationary phase and linearized reflection coefficients in weak anisotropic media: Geophysical Journal International, **158**, No. 1, 225–238.

Vavryčuk, V., and Pšenčík, I., 1998, PP-wave reflection coefficients in weakly anisotropic elastic media: Geophysics, **63**, No. 6, 2129–2141.